

Semileptonic decays of K and D mesons in $2 + 1$ flavor QCD

Elvira Gámiz
for FNAL/MILC collaboration



Fermi National Accelerator Laboratory

The XXVIII International Symposium on Lattice Field Theory

• Villasimius, Sardinia, Italy, June 15 (2010) •

1. Introduction: semileptonic decays

Extraction of CKM matrix elements

$$\frac{d}{dq^2} \Gamma(P_1 \rightarrow P_2 l \nu) \propto |V_{ab}|^2 |f_+^{P_1 \rightarrow P_2}(q^2)|^2 \quad q = p_{P_2} - p_{P_1}$$

1. Introduction: semileptonic decays

Extraction of CKM matrix elements

$$\frac{d}{dq^2} \Gamma(P_1 \rightarrow P_2 l \nu) \propto |V_{ab}|^2 |f_+^{P_1 \rightarrow P_2}(q^2)|^2 \quad q = p_{P_2} - p_{P_1}$$

CLEO-c, Besson et al PRD80 (2009)

Aubin et al. PRL94(2005)

$$|V_{cs}| f_+(0)^{D \rightarrow K} = 0.719(\pm 0.8\% \pm 0.7\%)$$

$$f_+(0)^{D \rightarrow K, latt} : 11\% \text{ error}$$

$$|V_{cd}| f_+(0)^{D \rightarrow \pi} = 0.150(\pm 3\% \pm 0.7\%)$$

$$f_+(0)^{D \rightarrow \pi, latt} : 10\% \text{ error}$$

BaBar, Aubert et al PRD76 (2007)

$$|V_{cs}| f_+(0)^{D \rightarrow K} = 0.717(\pm 0.8\% \pm 0.7 \pm 0.7\%) \text{ (last error from } B(D^0 \rightarrow K^- \pi^+))$$

* For D decays error in $|V_{cj}|$ dominated by lattice errors

* Testing lattice QCD: shape of the form factors

1. Introduction: semileptonic decays

Extraction of CKM matrix elements

$$\frac{d}{dq^2} \Gamma(P_1 \rightarrow P_2 l \nu) \propto |V_{ab}|^2 |f_+^{P_1 \rightarrow P_2}(q^2)|^2 \quad q = p_{P_2} - p_{P_1}$$

CLEO-c, Besson et al PRD80 (2009)

Aubin et al. PRL94(2005)

$$|V_{cs}| f_+(0)^{D \rightarrow K} = 0.719(\pm 0.8\% \pm 0.7\%)$$

$$f_+(0)^{D \rightarrow K, latt} : 11\% \text{ error}$$

$$|V_{cd}| f_+(0)^{D \rightarrow \pi} = 0.150(\pm 3\% \pm 0.7\%)$$

$$f_+(0)^{D \rightarrow \pi, latt} : 10\% \text{ error}$$

BaBar, Aubert et al PRD76 (2007)

$$|V_{cs}| f_+(0)^{D \rightarrow K} = 0.717(\pm 0.8\% \pm 0.7 \pm 0.7\%) \text{ (last error from } B(D^0 \rightarrow K^- \pi^+))$$

* For D decays error in $|V_{cj}|$ dominated by lattice errors

* Testing lattice QCD: shape of the form factors

Experimental average, Antonelli et al. (Flavianet), arXiv:1005.2323

$$|V_{us}| f_+(0)^{K \rightarrow \pi} = 0.2163(\pm 0.23\%)$$

$$f_+(0)^{K \rightarrow \pi, latt} : 0.6\% \text{ error}$$

1. Introduction: semileptonic decays

* Check unitarity in the first row of CKM matrix.

$$\Delta_{CKM} = |V_{ud}|^2 + |V_{us}|^2 + |V_{ub}|^2 - 1 = -0.0001(6) \quad \text{M. Antonelli et al,}$$

arXiv:1005.2323

fits to K_{l3}, K_{l2} exper. data and lattice results for $f_+(0)^{K \rightarrow \pi}$ and f_K/f_π

→ $\mathcal{O}(10 \text{ TeV})$ bound on the scale of new physics.

2. $D \rightarrow \pi$: Extraction of $|V_{cd}|$

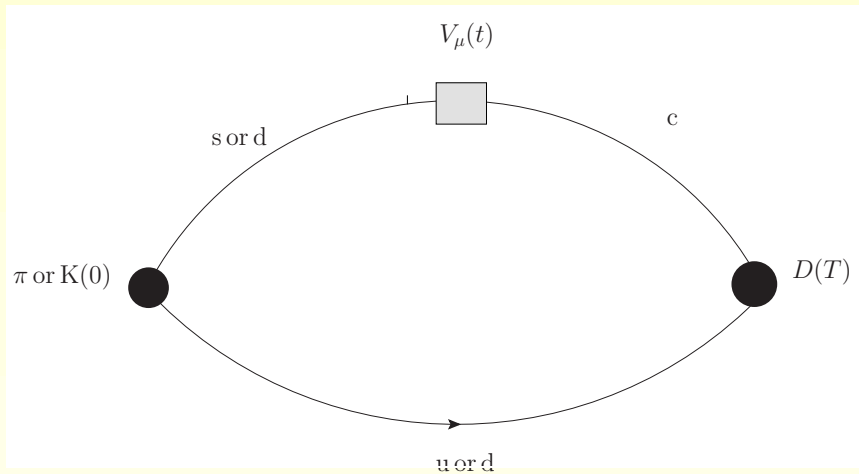
Validate method in D sem. decays

→ use same method for other processes like $B \rightarrow \pi l \nu$ or $B \rightarrow K l \bar{l}$

2. $D \rightarrow \pi$: Extraction of $|V_{cd}|$

Validate method in D sem. decays

→ use same method for other processes like $B \rightarrow \pi l \nu$ or $B \rightarrow K l \bar{l}$



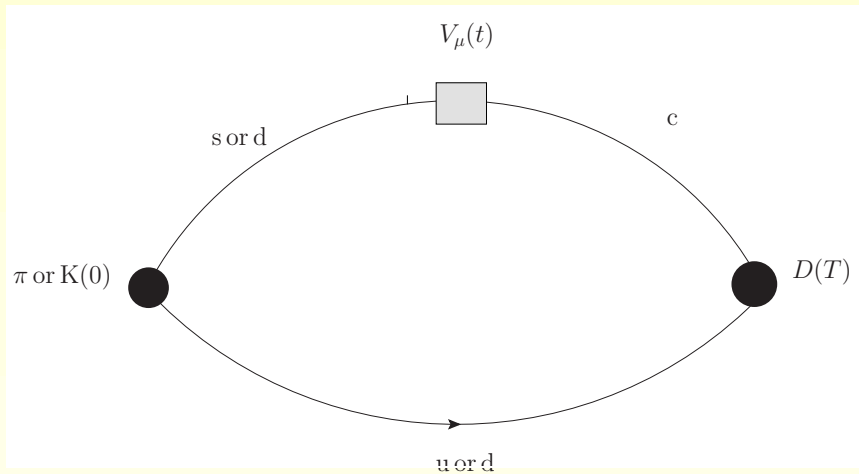
$$\langle P | V^\mu | D \rangle = f_+(q^2) \left[p_D^\mu + p_P^\mu - \frac{m_D^2 - m_P^2}{q^2} q^\mu \right] + f_0(q^2) \frac{m_D^2 - m_P^2}{q^2} q^\mu$$

* Work on D rest frame

2. $D \rightarrow \pi$: Extraction of $|V_{cd}|$

Validate method in D sem. decays

→ use same method for other processes like $B \rightarrow \pi l \nu$ or $B \rightarrow K l \bar{l}$



$$\langle P | V^\mu | D \rangle = f_+(q^2) \left[p_D^\mu + p_P^\mu - \frac{m_D^2 - m_P^2}{q^2} q^\mu \right] + f_0(q^2) \frac{m_D^2 - m_P^2}{q^2} q^\mu$$

* Work on D rest frame

A more convenient choice of parameters is

$$\langle P | V_\mu | D \rangle = \sqrt{2m_D} \left[v_\mu f_{\parallel}^{D \rightarrow P}(q^2) + p_{\perp \mu} f_{\perp}^{D \rightarrow P}(q^2) \right]$$

with $f_{\parallel}^{D \rightarrow P}(q^2) = \frac{\langle \pi | \mathcal{V}^0 | D \rangle}{\sqrt{2m_D}}$ and $f_{\perp}^{D \rightarrow P}(q^2) = \frac{\langle \pi | \mathcal{V}^i | D \rangle}{\sqrt{2m_D}} \frac{1}{p_\pi^i}$ (D rest frame)

2.1 Simulation details: Lattice actions

Sea quarks: $N_f = 2 + 1$ MILC configurations with improved staggered Asqtad u , d and s sea quarks, and improved glue

* Asqtad: Tree-level order a^2 effects removed
→ leading errors are $\mathcal{O}(\alpha_s a)$ $\mathcal{O}(a^4)$

Naik, NPB 1989; Lepage, PRD 1999; Bernard et al, PRD 1998

* One-loop Symanzik-improved gauge action: Weisz, NPB 1983; Curci et al., PLB 1983; Weisz and Wohlert, NPB 1984; Luscher and Weisz, PLB and CMP 1985; Alford et al., PLB 1995; Bernard et al., PRD 1998

2.1 Simulation details: Lattice actions

Sea quarks: $N_f = 2 + 1$ MILC configurations with improved staggered Asqtad u , d and s sea quarks, and improved glue

- * Asqtad: Tree-level order a^2 effects removed
→ leading errors are $\mathcal{O}(\alpha_s a)$ $\mathcal{O}(a^4)$

Naik, NPB 1989; Lepage, PRD 1999; Bernard et al, PRD 1998

- * One-loop Symanzik-improved gauge action: Weisz, NPB 1983; Curci et al., PLB 1983; Weisz and Wohlert, NPB 1984; Luscher and Weisz, PLB and CMP 1985; Alford et al., PLB 1995; Bernard et al., PRD 1998

Valence c : Fermilab action EI-Khadra et al, PRD 1997

- * Fermilab action: Clover with Fermilab interpretation via HQET
- ** Tune hopping parameter and clover coefficient to eliminate discretization effects through NLO

2.1 Simulation details: Lattice actions

Sea quarks: $N_f = 2 + 1$ MILC configurations with improved staggered Asqtad u , d and s sea quarks, and improved glue

- * Asqtad: Tree-level order a^2 effects removed
→ leading errors are $\mathcal{O}(\alpha_s a)$ $\mathcal{O}(a^4)$

Naik, NPB 1989; Lepage, PRD 1999; Bernard et al, PRD 1998

- * One-loop Symanzik-improved gauge action: Weisz, NPB 1983; Curci et al., PLB 1983; Weisz and Wohlert, NPB 1984; Luscher and Weisz, PLB and CMP 1985; Alford et al., PLB 1995; Bernard et al., PRD 1998

Valence c : Fermilab action EI-Khadra et al, PRD 1997

- * Fermilab action: Clover with Fermilab interpretation via HQET
- ** Tune hopping parameter and clover coefficient to eliminate discretization effects through NLO

Valence light quarks: Asqtad action.

2.1 Simulation details: Lattice actions

Improved vector currents.

* Rotate heavy quark field to remove $\mathcal{O}(1/m_c)$ errors:

$$\psi_c \rightarrow \Psi_c = \left(1 + ad_1 \vec{\gamma} \cdot \vec{D}_{lat} \right) \psi_c$$

** d_1 its fixed to its tadpole-improved tree-level value.

2.1 Simulation details: Lattice actions

Improved vector currents.

* Rotate heavy quark field to remove $\mathcal{O}(1/m_c)$ errors:

$$\psi_c \rightarrow \Psi_c = \left(1 + ad_1 \vec{\gamma} \cdot \vec{D}_{lat} \right) \psi_c$$

** d_1 its fixed to its tadpole-improved tree-level value.

Renormalization: Partially non-perturbative.

$$Z_{V_\mu}^{hl} = \rho_{V_\mu}^{hl} \sqrt{Z_V^{hh} Z_V^{ll}}$$

* Z_V^{hh} and Z_V^{ll} determined non-perturbatively

* $\rho_{V_\mu}^{hl}$ perturbative correction (one-loop). Small correction.

2.1 Simulation details: Parameters

	$\approx a$ (fm)	am_l/am_s	Volume	N_{conf}	$am_l^{valence}$
coarse	0.12	0.02/0.05	$20^3 \times 64$	2052	0.005, 0.007, 0.01,
		0.01/0.05	$20^3 \times 64$	2259	0.02, 0.03, 0.0415,
		0.007/0.05	$20^3 \times 64$	2110	0.05; 0.0349
		0.005/0.05	$24^3 \times 64$	2099	
fine	0.09	0.0124/0.031	$28^3 \times 96$	1996	0.0031, 0.0047, 0.0062,
		0.0062/0.031	$28^3 \times 96$	1946	0.0093, 0.0124, 0.031;
		0.00465/0.031	$32^3 \times 96$	983	0.0261
		0.0031/0.031	$40^3 \times 96$	1015	
superfine	0.06	0.0072/0.018	$48^3 \times 144$	593	0.0036, 0.0072, 0.0018,
		0.0036/0.018	$48^3 \times 144$	668	0.0025, 0.0054, 0.0160;
		0.0025/0.018	$56^3 \times 144$	800	0.0188
		0.0018/0.018	$64^3 \times 144$	826	

* Valence charm quark mass: tuned to physical value

* Current analysis: $m_l^{valence} = m_l^{sea}$

2.2 Correlation functions

Generate 3-point and 2-point correlation functions

$$C_{3,\mu}^{D \rightarrow \pi}(t, T; \vec{p}_\pi) = \sum_{\vec{x}, \vec{y}} e^{i\vec{p}_\pi \cdot \vec{y}} \langle \mathcal{O}_\pi(t_{source}, \vec{0}) V_\mu(t, \vec{y}) \mathcal{O}_D^\dagger(T, \vec{x}) \rangle$$

$$C_2^\pi(t; \vec{p}_\pi) = \sum_{\vec{x}} e^{i\vec{p}_\pi \cdot \vec{x}} \langle \mathcal{O}_\pi(t_{source}, \vec{0}) \mathcal{O}_\pi^\dagger(t, \vec{x}) \rangle$$

$$C_2^D(t) = \sum_{\vec{x}} \langle \mathcal{O}_D(t_{source}, \vec{0}) \mathcal{O}_D^\dagger(t, \vec{x}) \rangle$$

- * D rest frame: $\vec{p}_\pi = (0, 0, 0), (1, 0, 0), (1, 1, 0), (1, 1, 1), (2, 0, 0)$.
- * Randomizing spatial location of the sources \rightarrow decreases autocorrelations.
- * **Smearing**: D -meson interpolating operators are smeared with a $1S$ charmonium wavefunction.

2.2 Correlation functions

Generate 3-point and 2-point correlation functions

$$C_{3,\mu}^{D \rightarrow \pi}(t, T; \vec{p}_\pi) = \sum_{\vec{x}, \vec{y}} e^{i\vec{p}_\pi \cdot \vec{y}} \langle \mathcal{O}_\pi(t_{source}, \vec{0}) V_\mu(t, \vec{y}) \mathcal{O}_D^\dagger(T, \vec{x}) \rangle$$

$$C_2^\pi(t; \vec{p}_\pi) = \sum_{\vec{x}} e^{i\vec{p}_\pi \cdot \vec{x}} \langle \mathcal{O}_\pi(t_{source}, \vec{0}) \mathcal{O}_\pi^\dagger(t, \vec{x}) \rangle$$

$$C_2^D(t) = \sum_{\vec{x}} \langle \mathcal{O}_D(t_{source}, \vec{0}) \mathcal{O}_D^\dagger(t, \vec{x}) \rangle$$

- * D rest frame: $\vec{p}_\pi = (0, 0, 0), (1, 0, 0), (1, 1, 0), (1, 1, 1), (2, 0, 0)$.
 - * Randomizing spatial location of the sources \rightarrow decreases autocorrelations.
 - * **Smearing**: D -meson interpolating operators are smeared with a $1S$ charmonium wavefunction.
- # Build combinations of $C_3^{D \rightarrow \pi}(t, T)$ and $C_3^{D \rightarrow \pi}(t, T + 1)$ to suppress contributions from opposite parity (staggered artifacts) and excited states
- \rightarrow fit to a plateau or plateau + dominant oscillating contamination

2.3 Chiral and continuum extrapolation

Partially-quenched heavy-meson staggered ChPT Aubin & Bernard, PRD76(2007)

* Use complete NLO + analytic NNLO expressions.

$$f_{\parallel} = \frac{c_0}{f_{\pi}} \left[1 + \text{logs} + c_1 m_l + c_2 E_{\pi} + c_3 (E_{\pi})^2 + c_4 a^2 + \text{NNLO analy. terms} \right]$$
$$f_{\perp} = \frac{c'_0 g_{\pi}}{f_{\pi}} \left\{ \frac{1}{E_{\pi} + \Delta_l^* + \text{logs}} + \frac{1}{E_{\pi} + \Delta_l^*} \left[\text{logs} + c'_1 m_l + c'_2 E_{\pi} + c'_3 (E_{\pi})^2 + c'_4 a^2 + \text{NNLO analy. terms} \right] \right\}$$

** No sea quark mass dependence is included (m_s^{sea} similar in all ensembles and $m_l^{val.} = m_l^{sea}$)

** No a^4 term is included (only two lattice spacings).

** logs are known non-analytical functions of $m_{K,\pi}$ containing dominant taste-breaking effects

→ remove the dominant light discretization errors

2.3 Chiral and continuum extrapolation

- * **Checks:** extrapolated results for f_+ quite insensitive to NNNLO corrections

2.3 Chiral and continuum extrapolation

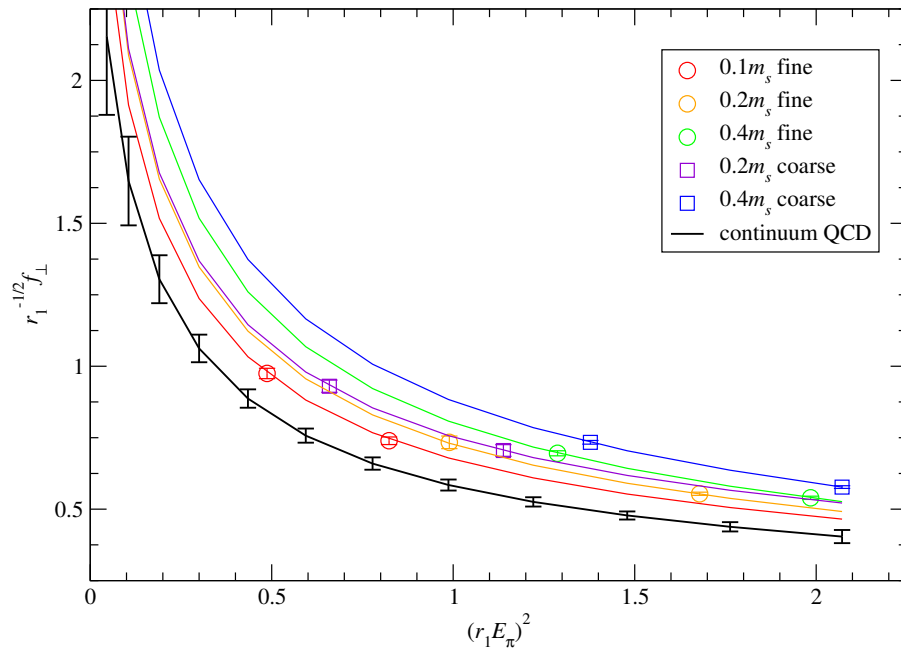
- * **Checks:** extrapolated results for f_+ quite insensitive to **NNLO** corrections
- * **Future plan:** Include also **heavy-quark** discretization errors from the action and the current to improve errors estimates
- ** Corrections given by higher order operators in the **HQET** expansion. Known functions of am_c included in the fits with $\mathcal{O}(1)$ coefficients to be determined by the fit.
 - incorporates power counting fixing hadronic scales more systematically

2.3 Chiral and continuum extrapolation

Preliminary results

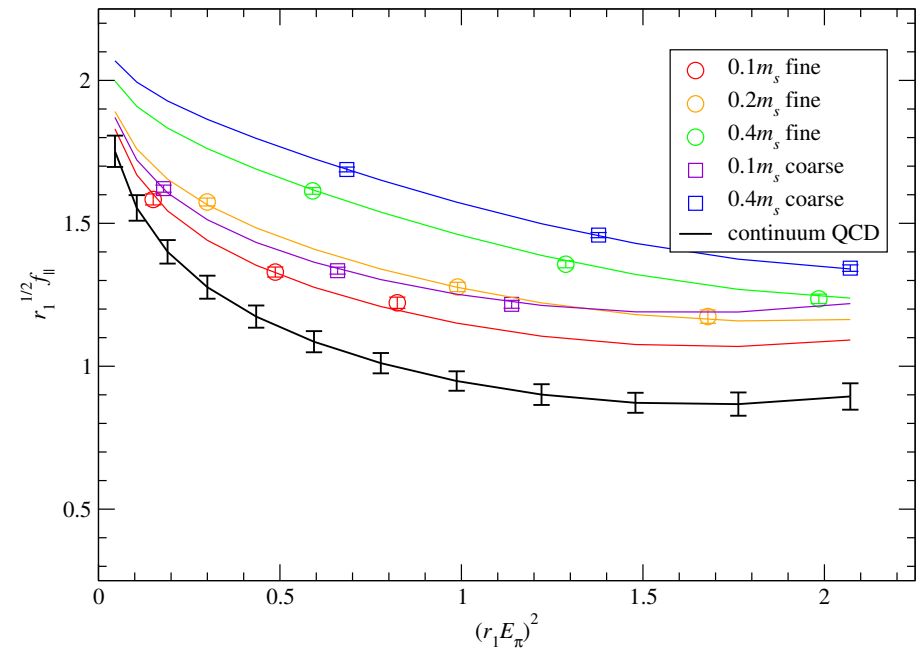
Chiral-continuum-energy extrap.-interp.

$$\chi^2/10 = 0.16$$



Chiral-continuum-energy extrapolation-interpolation

$$\chi^2/15 = 1.3$$

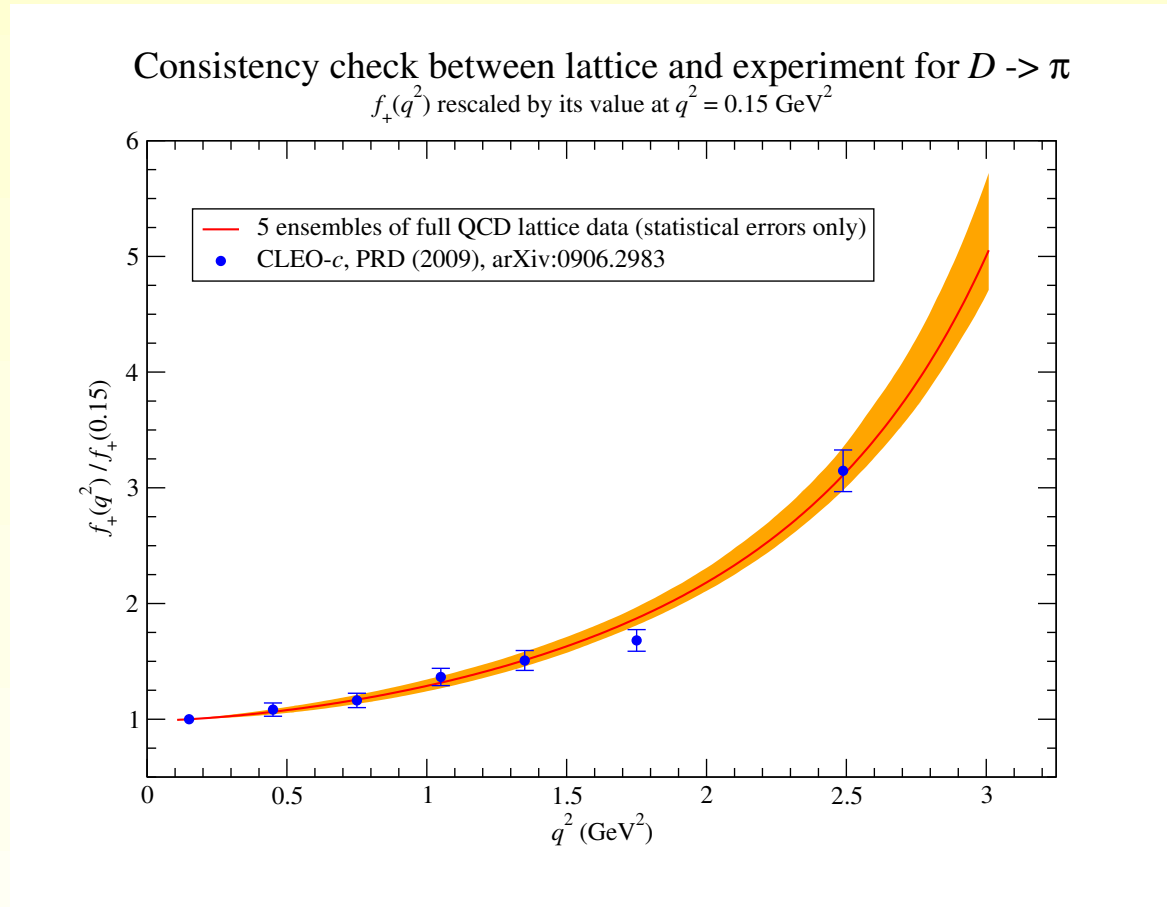


ChPT not reliable for $\chi_{\pi} = \frac{\sqrt{2}E_{\pi}}{4\pi f_{\pi}} > 1 \rightarrow \vec{p}_{\pi} = (1, 1, 1), (2, 0, 0)$ not used in the fits.

$\rho_{V_{\mu}}^{hl}$ factors not included yet in the renormalization.

2.4 Comparison with experimental data

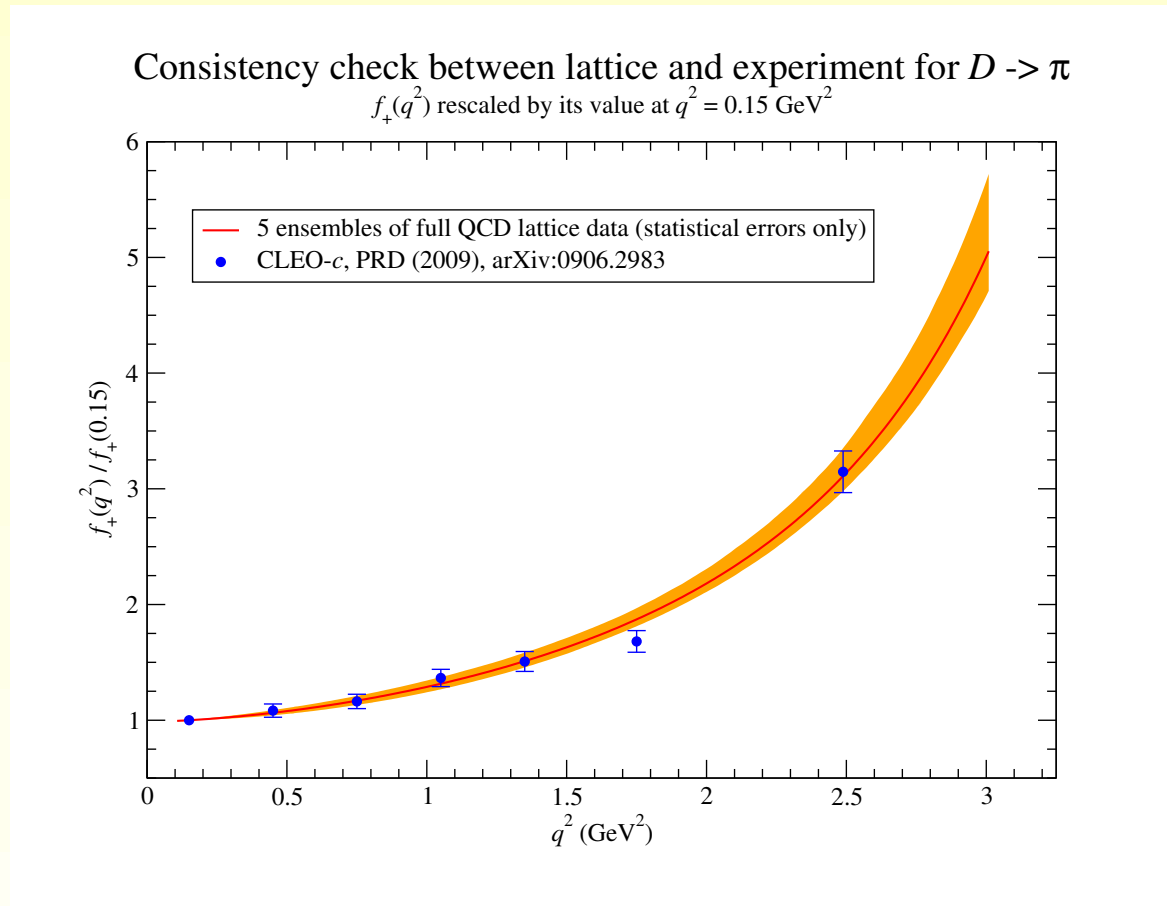
Preliminary results



Statistical errors for $f_+(0.15 \text{ GeV}^2)^{D \rightarrow \pi}$: $\simeq 5\%$

2.4 Comparison with experimental data

Preliminary results



Statistical errors for $f_+(0.15\text{GeV}^2)^{D \rightarrow \pi}$: $\simeq 5\%$

Plan: Use z -**expansion** to extract $|V_{ud}|$ in a model-independent way from a simultaneous fit of lattice and experimental data over q^2

z -**expansion** based on unitarity, analyticity, crossing symmetry, and heavy-quark symmetry

3.1. $K \rightarrow \pi l \nu$: Methodology

HPQCD method for semileptonic decays (see H. Na talk)

* In the continuum, the Ward identity ($S = \bar{d}s$)

$$q^\mu \langle \pi | V_\mu^{cont.} | K \rangle = (m_s - m_q) \langle \pi | S^{cont} | K \rangle$$

relates matrix elements of vector and scalar currents.

3.1. $K \rightarrow \pi l \nu$: Methodology

HPQCD method for semileptonic decays (see H. Na talk)

* In the continuum, the Ward identity ($S = \bar{d}s$)

$$q^\mu \langle \pi | V_\mu^{cont.} | K \rangle = (m_s - m_q) \langle \pi | S^{cont.} | K \rangle$$

relates matrix elements of vector and scalar currents. In the lattice

$$q^\mu \langle \pi | V_\mu^{lat.} | K \rangle Z = (m_s - m_q) \langle \pi | S^{lat.} | K \rangle$$

Using it together with

$$\langle \pi | V^\mu | K \rangle = f_+(q^2) \left[p_K^\mu + p_\pi^\mu - \frac{m_K^2 - m_\pi^2}{q^2} q^\mu \right] + f_0(q^2) \frac{m_K^2 - m_\pi^2}{q^2} q^\mu$$

→ substitute the 3-point function with a V_μ insertion by a 3-point function with a S insertion

$$f_0(q^2) = \frac{m_s - m_q}{m_K^2 - m_\pi^2} \langle \pi | S | K \rangle_{q^2}$$

3.1. $K \rightarrow \pi l \nu$: Methodology

HPQCD method for semileptonic decays (see H. Na talk)

* In the continuum, the Ward identity ($S = \bar{d}s$)

$$q^\mu \langle \pi | V_\mu^{cont.} | K \rangle = (m_s - m_q) \langle \pi | S^{cont.} | K \rangle$$

relates matrix elements of vector and scalar currents. In the lattice

$$q^\mu \langle \pi | V_\mu^{lat.} | K \rangle Z = (m_s - m_q) \langle \pi | S^{lat.} | K \rangle$$

Using it together with

$$\langle \pi | V^\mu | K \rangle = f_+(q^2) \left[p_K^\mu + p_\pi^\mu - \frac{m_K^2 - m_\pi^2}{q^2} q^\mu \right] + f_0(q^2) \frac{m_K^2 - m_\pi^2}{q^2} q^\mu$$

→ substitute the 3-point function with a V_μ insertion by a 3-point function with a S insertion

$$f_0(q^2) = \frac{m_s - m_q}{m_K^2 - m_\pi^2} \langle \pi | S | K \rangle_{q^2} \implies f_+(0) = f_0(0) = \frac{m_s - m_q}{m_K^2 - m_\pi^2} \langle S \rangle_{q^2=0}$$

3.1. Methodology

Advantages of the method:

- * No need of renormalization factors Z .
- * Need less inversions than the traditional double ratio method.
- * S currents used are local.

3.1. Methodology

Advantages of the method:

- * No need of renormalization factors Z .
- * Need less inversions than the traditional double ratio method.
- * S currents used are local.

Downside: can get $f_+(q^2)$ only at $q^2 = 0$.

3.2. Test run: simulation details

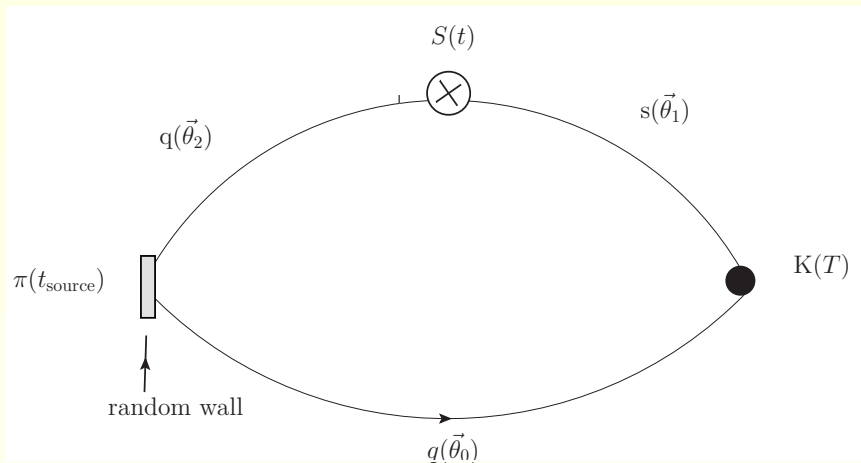
- # Sea quarks: $N_f = 2 + 1$ MILC configurations with improved staggered Asqtad u , d and s sea quarks, and improved glue
- # Valence quarks: Hisq action E. Follana et al, HPQCD coll., Phys.Rev.D75 (2007)
- * No tree level a^2 errors (Asqtad). Highly reduce $\mathcal{O}(a^2\alpha_s)$ errors.

3.2. Test run: simulation details

Sea quarks: $N_f = 2 + 1$ MILC configurations with improved staggered Asqtad u , d and s sea quarks, and improved glue

Valence quarks: Hisq action E. Follana et al, HPQCD coll., Phys.Rev.D75 (2007)

* No tree level a^2 errors (Asqtad). Highly reduce $\mathcal{O}(a^2\alpha_s)$ errors.



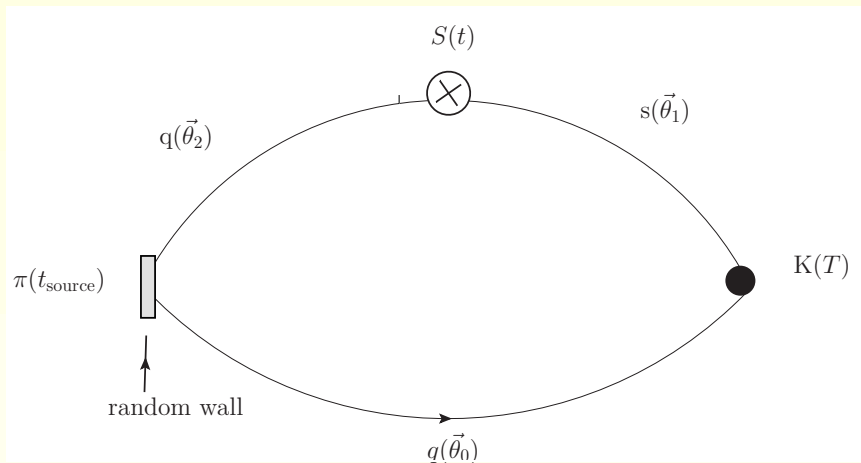
* Random wall sources: reduce stat. errors by a factor of 2-3.

3.2. Test run: simulation details

Sea quarks: $N_f = 2 + 1$ MILC configurations with improved staggered Asqtad u , d and s sea quarks, and improved glue

Valence quarks: Hisq action E. Follana et al, HPQCD coll., Phys.Rev.D75 (2007)

* No tree level a^2 errors (Asqtad). Highly reduce $\mathcal{O}(a^2\alpha_s)$ errors.



* Random wall sources: reduce stat. errors by a factor of 2-3.

* Twisted boundary conditions: allow to inject arbitrary momentum and simulate at $q^2 = 0$ directly.

** Momentum injected on the K : $\vec{\theta}_0 = \vec{\theta}_2 = 0, \vec{\theta}_1 \neq 0$ $\vec{p}_K = \vec{\theta}_1 \frac{\pi}{L}$

** Momentum injected on the π : $\vec{\theta}_0 = \vec{\theta}_1 = 0, \vec{\theta}_2 \neq 0$ $\vec{p}_\pi = \vec{\theta}_2 \frac{\pi}{L}$

3.2. Test run: simulation details

$\approx a$ (fm)	am_l^{sea}/am_s^{sea}	N_{conf}	$N_{sources}$	$am_s^{valence}$	$am_l^{valence}$
0.12	0.010/0.050	592	4	0.0546	0.010
0.09	0.0062/0.031	551	4	0.0366	0.0062

Generate $C_3^{K \rightarrow \pi}(t, T; \vec{p}_{\pi/K})$ for $T = 18 - 22$ for coarse lattice and $T = 27 - 30$ for fine lattice.

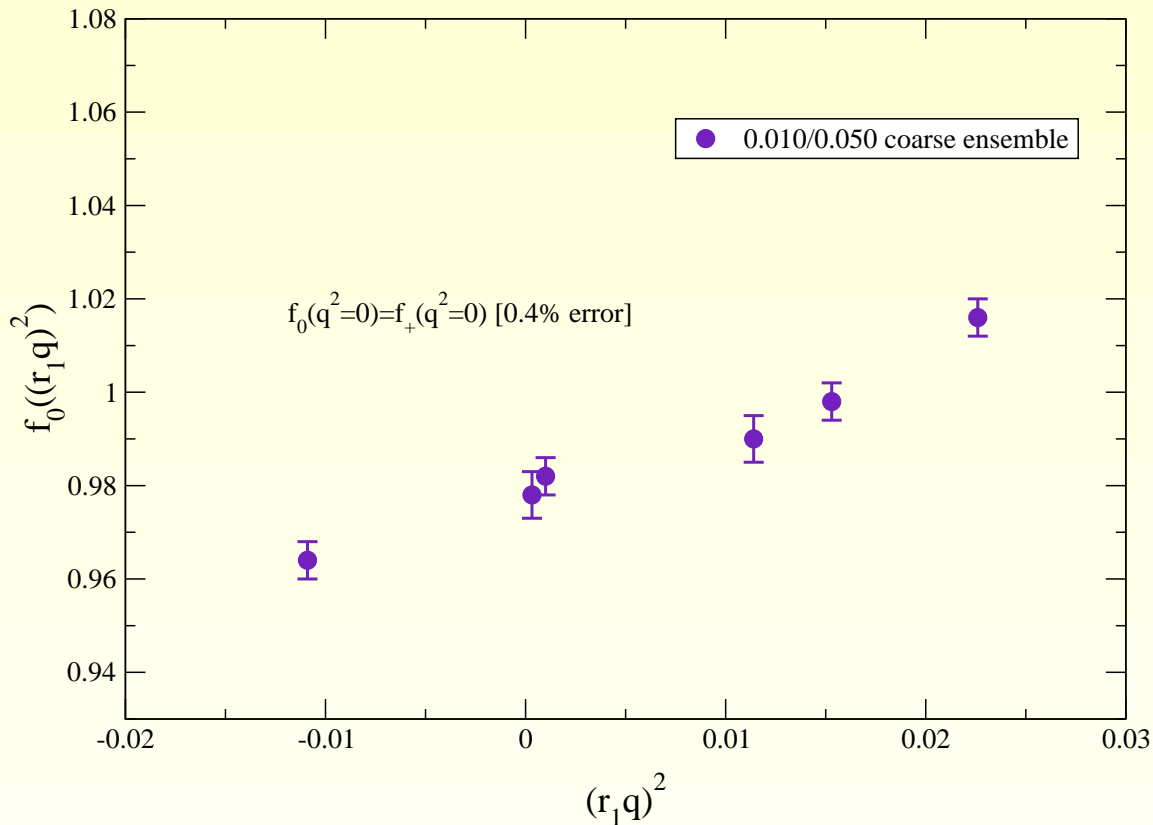
3.2. Test run: simulation details

$\approx a$ (fm)	am_l^{sea}/am_s^{sea}	N_{conf}	$N_{sources}$	$am_s^{valence}$	$am_l^{valence}$
0.12	0.010/0.050	592	4	0.0546	0.010
0.09	0.0062/0.031	551	4	0.0366	0.0062

- # Generate $C_3^{K \rightarrow \pi}(t, T; \vec{p}_{\pi/K})$ for $T = 18 - 22$ for coarse lattice and $T = 27 - 30$ for fine lattice.
- # **Fit** combinations of 3-point functions with $T = 19 - 20$ for coarse and $T = 28 - 29$ for fine, together with corresponding 2-point π and K functions.
- * Fit to ground state + dominant oscillating for central values of 3-point amplitudes.
- * Checking stability: Fit to ground state and keeping dependence on oscillating and excited states (up to 4 exponentials).

3.2. Test run: simulating at $q^2 \sim 0$

Dependence of the scalar form factor on q^2



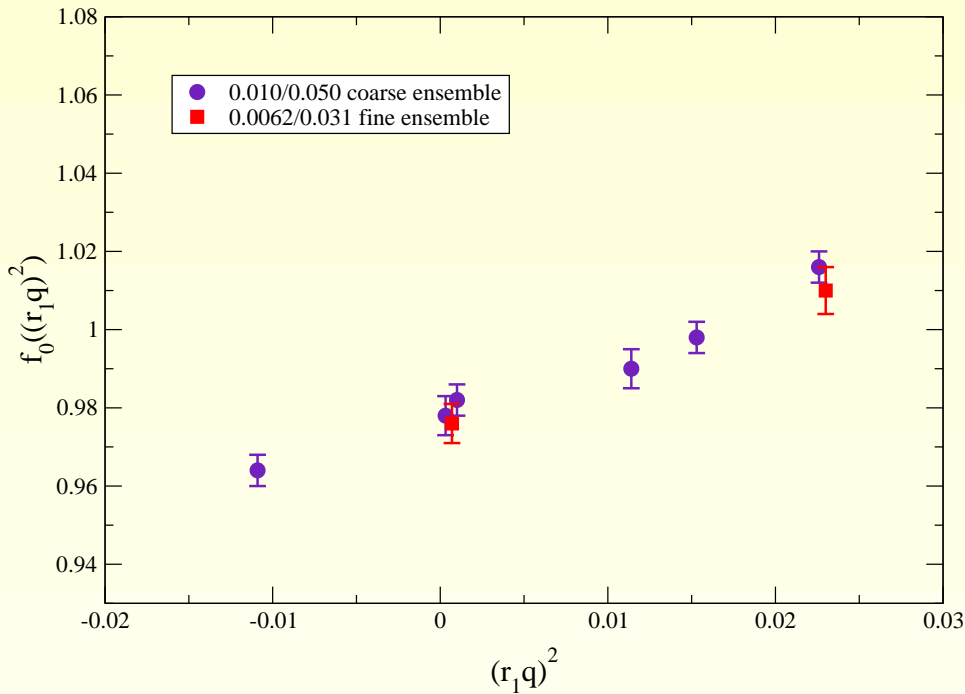
$ \vec{\theta}_1 $	$ \vec{\theta}_2 $	q^2
0	0	0.0227(3)
0	0.7295	0.0011(4)
0.7295	0	0.0153(3)
0	0.9105	-0.0109(5)
0.9105	0	0.0114(5)
1.2876	0	0.0003(3)

Goal: Eliminate uncertainty in q^2 interpolation (minimum value of $|(r_1 q)^2|$ available with periodic boundary conditions is $\simeq -0.104$)

$f_+(q^2 \simeq 0)$ calculated with $\sim 0.4\%$ statistical error (momentum in π).
4 times more configurations available! \rightarrow 0.2-0.3% stat. error

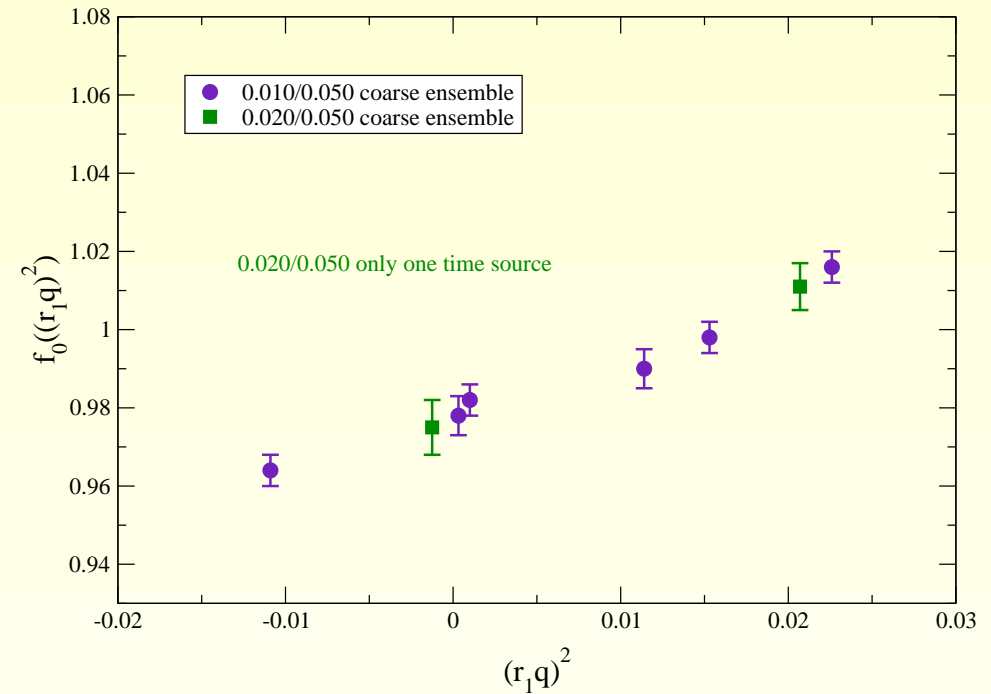
3.3. Test run: discretization and sea quark mass effects

Comparison of coarse ($a=0.12$ fm) and fine ($a=0.09$ fm) ensembles



Comparison of sea light quark masses $0.4m_s$ and $0.2m_s$

(on coarse ($a=0.12$ fm) lattice)



- # Discretization errors: negligible after extrapolation to the continuum.
- # Sea quark mass effects: negligible after extrapolation to the physical point.

3.4. Future plans: **Hisq** valence quarks

- # Use full **MILC** statistics for medium-coarse ($a \simeq 0.15 \text{ fm}$), coarse ($a \simeq 0.12 \text{ fm}$), and fine ($a \simeq 0.09 \text{ fm}$) ensembles.
- * $N_{conf.} \simeq 2000$ in coarse, $N_{conf.} \simeq 1000 - 2000$ in fine, and $N_{conf.} \simeq 600$ in medium-coarse.
- * At least 4 different sea quark masses for coarse, fine, and medium-coarse available.

3.4. Future plans: Hisq valence quarks

- # Use full MILC statistics for medium-coarse ($a \simeq 0.15 \text{ fm}$), coarse ($a \simeq 0.12 \text{ fm}$), and fine ($a \simeq 0.09 \text{ fm}$) ensembles.
 - * $N_{conf.} \simeq 2000$ in coarse, $N_{conf.} \simeq 1000 - 2000$ in fine, and $N_{conf.} \simeq 600$ in medium-coarse.
 - * At least 4 different sea quark masses for coarse, fine, and medium-coarse available.
- # Use (partially quenched) Staggered ChPT to extrapolate to the continuum and the physical light masses (valence strange mass tuned to the physical one)
 - * NLO ($\mathcal{O}(p^4)$) including taste-changing effects plus NNLO ($\mathcal{O}(p^6)$) continuum ChPT

3.4. Future plans: **Hisq** valence quarks

- # Use full **MILC** statistics for medium-coarse ($a \simeq 0.15 \text{ fm}$), coarse ($a \simeq 0.12 \text{ fm}$), and fine ($a \simeq 0.09 \text{ fm}$) ensembles.
 - * $N_{conf.} \simeq 2000$ in coarse, $N_{conf.} \simeq 1000 - 2000$ in fine, and $N_{conf.} \simeq 600$ in medium-coarse.
 - * At least 4 different sea quark masses for coarse, fine, and medium-coarse available.
- # Use (partially quenched) Staggered **ChPT** to extrapolate to the continuum and the physical light masses (**valence strange mass** tuned to the **physical** one)
 - * **NLO** ($\mathcal{O}(p^4)$) including taste-changing effects plus **NNLO** ($\mathcal{O}(p^6)$) continuum **ChPT**
- # **Statistical errors:** 0.3-0.2%
- # **Analysis of systematic errors:**
 - * Chiral and continuum extrap.: one of the dominant uncertainties
 - * Tuning of bare quark masses
 - * Finite volume effects

4. Conclusions and future prospects

- # $D \rightarrow \pi l \nu$: Complete analysis adding 2 coarse ensembles, 1 fine ensemble, and 1/2 superfine ensembles.
- * Add $m_l^{val.} \neq m_l^{sea}$: will help especially with $f_{||}$ extrapolation.
- * Use **z-expansion** to combine lattice and experimental data.
- * Updated treatment of correlations **Bernard et al. PRD80 (2009)**.
- * Incorporates known functional forms for higher order **heavy-quark discretization** effects in the chiral-continuum extrapolation.

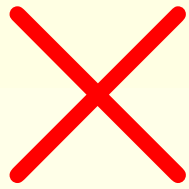
4. Conclusions and future prospects

Projected error budget for $f_+(0)^{D \rightarrow \pi}$

source	error (%)	comments/improvements
Stat. + χ PT	5	better when including $a = 0.06$ fm, more m_l^{val}
$g_{D^* D \pi}$	2.2	=
r_1	1.5	f_π
\hat{m}	0.5	m_π, m_K
m_s	2.0	=
m_c	0.2	updated κ_c
HQ	3.9	better estimate from chir+cont fits
Z_V	0.7	statist. dominated
ρ	0.7	pert. error
$L^3 < \infty$	0.5	ChPT
Sys.	5.3	
Total	7.3	(previous error 11% Aubin et al. PRL94(2005))

4. Conclusions and future prospects

- # $D \rightarrow \pi l \nu$: Complete analysis adding 2 coarse ensembles, 1 fine ensemble, and 1/2 superfine ensembles.
 - * Add $m_l^{val.} \neq m_l^{sea}$: will help especially with f_{\parallel} extrapolation.
 - * Use **z-expansion** to combine lattice and experimental data.
 - * Updated treatment of correlations **Bernard et al. PRD80 (2009)**.
 - * Incorporates known functional forms for higher order **heavy-quark discretization** effects in the chiral-continuum extrapolation.
- # $D \rightarrow K l \nu$. Expect similar errors.

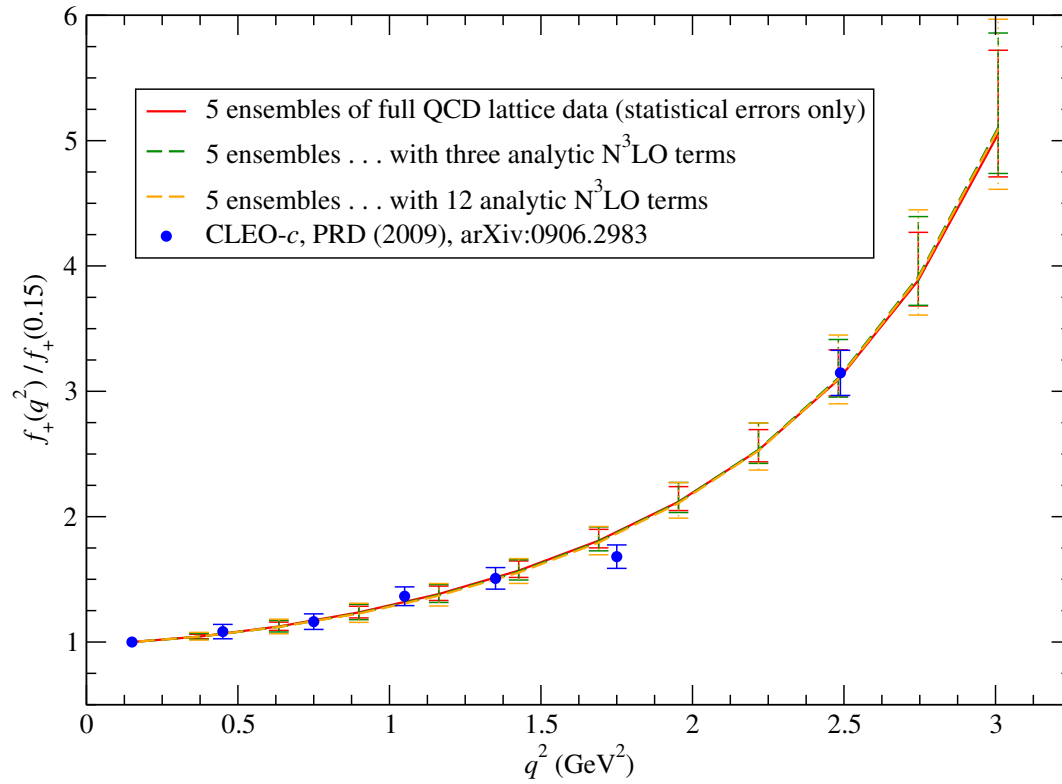


Iterative Super Average

$$\begin{aligned}
 \bar{C}_{3pt}^{K \rightarrow \pi}(t, T) &= \frac{e^{-E_\pi^{(0)} t} e^{-m_K^{(0)}(T-t)}}{8} \\
 &\times \left[\frac{C_{3pt}^{K \rightarrow \pi}(t, T)}{e^{-E_\pi^{(0)} t} e^{-m_K^{(0)}(T-t)}} + \frac{C_{3pt}^{K \rightarrow \pi}(t, T+1)}{e^{-E_\pi^{(0)}(t)} e^{-m_K^{(0)}(T+1-t)}} \right. \\
 &+ \frac{2 C_{3pt}^{K \rightarrow \pi}(t+1, T)}{e^{-E_\pi^{(0)}(t+1)} e^{-m_K^{(0)}(T-t-1)}} + \frac{2 C_{3pt}^{K \rightarrow \pi}(t+1, T+1)}{e^{-E_\pi^{(0)}(t+1)} e^{-m_K^{(0)}(T-t)}} \\
 &+ \left. \frac{C_{3pt}^{K \rightarrow \pi}(t+2, T)}{e^{-E_\pi^{(0)}(t+2)} e^{-m_K^{(0)}(T-t-2)}} + \frac{C_{3pt}^{K \rightarrow \pi}(t+2, T+1)}{e^{-E_\pi^{(0)}(t+2)} e^{-m_K^{(0)}(T-t-1)}} \right] \\
 &\approx A_\mu^{00} e^{-E_\pi^{(0)} t} e^{-m_K^{(0)}(T-t)} \\
 &+ (-1)^T A_\mu^{11} e^{-E_\pi^{(1)} t} e^{-m_K^{(1)}(T-t)} \left(\frac{\Delta m_K}{2} \right) \\
 &+ \mathcal{O}(\Delta E_\pi^2, \Delta E_\pi \Delta m_K, \Delta m_K^2)
 \end{aligned}$$

Consistency check between lattice and experiment for $D \rightarrow \pi$

$f_+(q^2)$ rescaled by its value at $q^2 = 0.15 \text{ GeV}^2$



$K \rightarrow \pi l \nu$: extraction of $|V_{us}|$

$K \rightarrow \pi l \nu$: extraction of $|V_{us}|$

Look for new physics effects in the comparison of $|V_{us}|$ from helicity suppressed $K_{\mu 2}$ versus helicity allowed $K_{l 3}$

$$R_{\mu 23} = \left(\frac{f_K / f_\pi}{f_+(0)} \right) \times \text{experim. data on } K_{\mu 2} \pi_{\mu 2} \text{ and } K_{l 3}$$

- * In the SM $R_{\mu 23} = 1$. Not true for some BSM theories (for example, charged Higgs)
- * Current value $R_{\mu 23} = 0.999(7)$, limited by lattice inputs.